CORA Cork Open Research Archive
Cartlann Taighde Oscailte Chorcaí

Title	Optical reflectance of solution processed quasi-superlattice ZnO and Al-doped ZnO (AZO) channel materials
Authors	Buckley, Darragh;McCormack, Robert;O'Dwyer, Colm
Publication date	2017-03-24
Original Citation	Buckley, D., McCormack, R. and O'Dwyer, C. (2017) 'Optical reflectance of solution processed quasi-superlattice ZnO and Al-doped ZnO (AZO) channel materials', Journal of Physics D - Applied Physics, 50, 16LT01 (7pp). doi:10.1088/1361-6463/aa6559
Type of publication	Article (peer-reviewed)
Link to publisher's version	10.1088/1361-6463/aa6559
Rights	© 2017 IOP Publishing Ltd. Original content from this work may be used under the terms of the Creative Commons Attribution 3.0 licence. Any further distribution of this work must maintain attribution to the author(s) and the title of the work, journal citation and DOI. - https://creativecommons.org/licenses/by/3.0/
Download date	2026-11-06 17:49:07
Item downloaded from	https://hdl.handle.net/10468/3894

UCC
University College Cork, Ireland
Coláiste na hOllscoile Corcaigh

IOPscience iopscience.iop.org

Home Search Collections Journals About Contact us My IOPscience

Optical reflectance of solution processed quasi-superlattice ZnO and Al-doped ZnO (AZO) channel materials

This content has been downloaded from IOPscience. Please scroll down to see the full text.

2017 J. Phys. D: Appl. Phys. 50 16LT01

(http://iopscience.iop.org/0022-3727/50/16/16LT01)

View the table of contents for this issue, or go to the journal homepage for more

Download details:

IP Address: 143.239.102.147
This content was downloaded on 04/04/2017 at 10:11

Please note that terms and conditions apply.

You may also be interested in:

Tuning of refractive index in Al-doped ZnO films by rf-sputtering using oblique angle deposition
E A Martín-Tovar, E Denis-Alcocer, E Chan y Díaz et al.

Highly transparent and reproducible nanocrystalline ZnO and AZO thin films grown by room temperature pulsed-laser deposition on flexible Zeonor plastic substrates
Saikumar Inguva, Rajani K Vijayaraghavan, Enda McGlynn et al.

Highly transparent and conductive Al-doped ZnO nanoparticulate thin films using direct write processing
S Vunnam, K Ankireddy, J Kellar et al.

Correlation between the electrical and structural properties of aluminium-doped ZnO thin films obtained by direct current magnetron sputtering
L Avril, Ph Guaino, F Maseri et al.

Pulsed laser deposited indium tin oxides as alternatives to noble metals in the near-infrared region
Xu Fang, C L Mak, Shiyu Zhang et al.

Li induced enhancement in c-axis orientation and its effect on structural, optical, and electrical properties of ZnO thin films
Dilawar Ali, M Z Butt, Bilal Arif et al.

The 2016 oxide electronic materials and oxide interfaces roadmap
M Lorenz, M S Ramachandra Rao, T Venkatesan et al.

Investigation of ZnO/Al/ZnO multilayers as transparent conducting coatings
M F Al-Kuhaili, M A Al-Maghrabi, S M A Durrani et al.

OPEN ACCESS
IOP Publishing

Letters
Journal of Physics D: Applied Physics

J. Phys. D: Appl. Phys. **50** (2017) 16LT01 (7pp)
https://doi.org/10.1088/1361-6463/aa6559

Letter

Optical reflectance of solution processed quasi-superlattice ZnO and Al-doped ZnO (AZO) channel materials

Darragh Buckley[1], **Robert McCormack**[1] **and Colm O'Dwyer**[1,2]

[1] Department of Chemistry, University College Cork, Cork T12 YN60, Ireland
[2] Micro-nano Systems Centre, Tyndall National Institute, Lee Maltings, Cork T12 R5CP, Ireland

E-mail: c.odwyer@ucc.ie

Received 22 January 2017, revised 28 February 2017
Accepted for publication 8 March 2017
Published 24 March 2017

Invited by Yue Kuo

Abstract

The angle-resolved reflectance of high crystalline quality, *c*-axis oriented ZnO and AZO single and periodic quasi-superlattice (QSL) spin-coated TFT channels materials are presented. The data is analysed using an adapted model to accurately determine the spectral region for optical thickness and corresponding reflectance. The optical thickness agrees very well with measured thickness of 1–20 layered QSL thin films determined by transmission electron microscopy if the reflectance from lowest interference order is used. Directional reflectance for single layers or homogeneous QSLs of ZnO and AZO channel materials exhibit a consistent degree of anti-reflection characteristics from 30 to 60° (~10–12% reflection) for thickness ranging from ~40 nm to 500 nm. The reflectance of AZO single layer thin films is <10% from 30 to 75° at 514.5 nm, and <6% at 632.8 nm from 30–60°. The data show that ZnO and AZO with granular or periodic substructure behave optically as dispersive, continuous thin films of similar thickness, and angle-resolved spectral mapping provides a design rule for transparency or refractive index determination as a function of film thickness, substructure (dispersion) and viewing angle.

Keywords: thin films, ZnO, AZO, reflectance, solution processed, TFT

S Supplementary material for this article is available online

(Some figures may appear in colour only in the online journal)

Introduction

Transparent conductive oxides (TCOs) are important materials due to their ability to have controllable conductivity and carrier mobility, while maintaining high optical transparency [1]. The trade-off between optical and electrical conductivity around the plasma frequency has motivated research into controlled and graded porosity in materials and structures to offset transparency loss in conductive oxides [2–6]. Metal oxide TCOs lead to the use of oxide semiconductors in many key optoelectronic devices such as TFTs [7], photovoltaics [8], solar cells [9] and electrochromics [10]. In particular, zinc oxide (ZnO) attracted the initial attention in this area due to its wide, direct band gap (E_g ~ 3.3 eV at 300 K) [11] and a crystal lattice that can be interstitially doped [12].

Currently, the semiconducting material used most in the area of optoelectronics is indium tin oxide (ITO), particularly in flat-panel displays [13]. This is due to its wide band gap

Original content from this work may be used under the terms of the Creative Commons Attribution 3.0 licence. Any further distribution of this work must maintain attribution to the author(s) and the title of the work, journal citation and DOI.

 © 2017 IOP Publishing Ltd Printed in the UK

(>3 eV), low electrical resistivity ($\leqslant 10^{-4}\,\Omega$ cm) and absorption coefficient of 10^4 cm^{-1} in the near-UV and visible range [14]. However, there is an interest in developing metal oxide semiconductors to replace ITO, such as ZnO [15], In-doped ZnO (IZO), In–Ga–Zn–O (IGZO) and Al-doped ZnO (AZO) [16]. For AZO, the composition avoids expensive and resource-critical indium due to the higher relative abundance in the Earth's crust (75 ppm for Zn opposed to 0.16 ppm for In) [17].

ZnO can be grown as a polycrystalline material at low temperatures or even room temperature [18] and has a larger exciton binding energy (~60 meV) than other wide band gap semiconductors [19]. ZnO is also attractive as it can be grown by a multitude of methods such as rf sputtering [18], pulsed laser deposition [20] and solution-processed methods [21], providing quite good TFT performance compared to primary amorphous oxide semiconductor technologies [22, 23]. However, on its own, ZnO does not meet the electrical performance standards set by ITO due to a higher resistivity from a lower majority carrier concentration [17, 24], but important advances are being made in post-deposition annealing to significantly improve and control its response [17]. In order to improve its electrical properties and reduce sheet resistance and resistivity, while also maintaining a low-cost, non-toxic and stable material, ZnO can be doped with trivalent electron donor metals such as Al or Ga to ensure high free-carrier mobility and transparency via the Burnstein–Moss shift that gives metal oxides their useful attributes [25]. Modulating the carrier concentration of a material will also affect its optical properties, specifically the plasma frequency, dielectric constant or refractive index [26]. Introducing a dopant such as Al into the crystal lattice can also produce tensile stress in the crystal lattice. These stresses can cause band-gap widening and alter the optical properties of the material [27]. In solution-processing of single and multi-layered oxides, polycrystallinity and a degree of porosity also modify the effective refractive index and overall film resistivity [28–30]. Solution-processed TCOs [31] can be doped from precursor mixtures and annealing protocols without significant changes to structure, allowing the alteration of the free-electron concentration and thus the optical properties. This makes these materials optically tunable while being structurally stable [32].

Optical reflectivity is a vital characteristic in optoelectronics, particularly in transparent TFT devices and solar cells that require control in anti-reflection, absorption or directional reflectance. For 'standard' TFTs, correlating the true optical thickness to actual thickness at near-normal incidence helps to correlate optical conductivity to electrical resistivity and morphology for a range of TFT material types. In multi-layered oxide films, or those that have porous, granular or QSL substructure, reflectance is subject to dispersion and variation of effective refractive index. When substructure is used to modify or control electrical properties such as resistivity or sheet resistance in metal oxide channel materials for TFTs, accurate determination of optical thickness and reflectance is critical. This is especially true for superlattice or multi-layered films of nanoscale (subwavelength) thickness, where correlation of the optical thickness to the actual thickness is required in tandem with defined optical conductivity.

In this work we show an adapted method to accurately determine the optical thickness for dispersive QSL solution processed ZnO and AZO thin film TFT channel materials directly from optical reflectance. The results demonstrate that dispersion caused by the multi-layered substructure in the periodic QSL necessitates a low interference order to correctly determine the optical thickness, particularly for quasi-superlattice or thicker films. Furthermore, we show that, in general, multilayered or homogeneous QSLs of metal oxides with a single composition for TFTs are dispersive materials that behave as continuous thin films with thickness controlled by cumulative spin-coating. The angle-resolved reflectance for single layers and QSLs is also determined for ZnO and doped AZO TFT materials, and provides a design rule for transparency determination as a function of film thickness. Importantly, the wavelength for optical thickness determination relates to the lowest interference order and not necessarily the highest transparency for oxide thin films. Angle-resolved spectral mapping of reflectance identifies a design rule for such materials to define maximum transparency and correlate it to effective optical thickness.

Experimental

ZnO and Al:ZnO thin film and multilayer formation

A 0.75M solution of zinc acetate dihydrate [$Zn(CH_3COO)_2 \cdot 2H_2O$] dissolved in 2-methoxyethanol [$CH_3OCH_2CH_2OH$] was prepared in order to deposit ZnO thin films. A solution of monoethanolamine was added to this zinc acetate solution to act as a stabilising agent. The molar ratio of the monoethanolamine solution to the zinc acetate solution was kept at 1:1. In order to prepare Al:ZnO (AZO) films of 5 mol% Al, an Al-solution was prepared by dissolving 0.1407 g of aluminium nitrate-nonahydrate [$Al(NO_3)_3 \cdot 9H_2O$] in 10 ml of 2-methoxyethanol. This solution was added to the 0.75 M zinc acetate solution and stirred for 2 h at 60 °C.

All thin films samples were deposited onto p-type silicon wafers cleaved to 2 cm × 2 cm in size. Prior to deposition, substrates were cleaned via sonication in acetone, IPA and DI water and then received a 30 min UV-ozone treatment using a Novascan UV ozone system. Films were deposited from liquid precursors using a SCS G3 desktop spin coater. The appropriate solution was added dropwise to the substrate and spun at 3000 rpm for 30 s, including a 5 s ramp time. Following this, samples were dried for 5 min between 250 and 270 °C in an open-air convection oven. This deposition process can be repeated as many times as desired before samples undergo a final annealing treatment at 300 °C for 1 h.

Electron microscopy

To investigate the thickness of prepared ZnO and AZO films, transmission electron microscopy (TEM) was conducted on cross-sectioned lamellae. TEM analysis was conducted using a JEOL JEM-2100 TEM operating at 200 kV. Lamella from samples with 1, 5, 10 and 20 layers of ZnO and AZO were

prepared for TEM analysis by cross-sectioning using an FEI Helios Nanolab Dual Beam Focused-ion Beam (FIB) System.

Optical reflectance spectroscopy

Angle-resolved optical characterisation was conducted using an in-house constructed cage-mounted optical reflectance/transmission spectroscopy setup. The reflectivity was obtained at variable AOI using high precision 360° rotation mount and collection arm with constant path length. Samples were illuminated with a white tungsten halogen lamp collimated to a beam diameter of ~1–2 mm using optical fiber with an output spectral range from 360 to 2400 nm. The reflected light was collected using focusing optics into an Oceanoptics USB2000 + spectrometer (400–1000 nm range) which has an optical resolution of 1.5 nm. The reflected light was also collected in the same manner using an Oceanoptics NIRQuest512-2.5 to obtain the NIR reflectance spectra (1000–2500 nm range) which has an optical resolution of 6.3 nm. Reference spectra were acquired using an Au mirror (ThorLabs gold mirror PF10-03-M01) at each AOI investigated prior to sample data collection under identical conditions.

Both sets of thin film samples were measured at various angles of incidence with respect to the normal of the thin film surface in order to investigate the anti-reflection properties of the ZnO and AZO at various angles and wavelengths. Thin film samples with 1, 10 and 20 layers in both thin films sets were measured at three different angles of incidence, $\theta_i = 30°$, 60° and 75°. Full UV–NIR spectra (400–2500 nm) were acquired of all samples at an angle of incidence of 45°. Using these spectra, optical parameters for each film can be determined and the optical thickness calculated as a result. Background theory and full mathematical treatment for this analysis, including error analysis of optical thickness measurements determined from spectral data, is provided in the supplementary material (stacks.iop.org/JPhysD/50/16LT01/mmedia).

Results and discussion

ZnO and AZO thin-films and multilayered QSL films were spin-coated onto silicon wafers with 85 nm thermally grown SiO_2 and sequential film deposition was carried out following the cumulative drying and final annealing process for each layer (see Experimental), for both ZnO and AZO materials. FIB-sectioned TEM images of ZnO and AZO films are shown in figures 1(a) and (b), where very uniform thickness control is demonstrated. Further details on the chemical, structural and growth process for these films can be found elsewhere. All films exhibit very high crystal quality, and multilayered samples with 20 iterative coated layers are predominantly [0 0 0 2] oriented along the *c*-axis direction of the unit cell, shown in figure 1(c). Multilayered QSL ZnO and AZO films, shown in figure 1, comprise a periodic quasi-superlattice of apparently granular and dense layers with consistent periodic thickness of 35–40 nm for ZnO and 15–18 nm for AZO. Banger *et al* recently demonstrated IZO TFTs with high field-effect mobility [7]. Single layers of their IZO thin films look similar in morphology to the ZnO and AZO layers we show here, but their system used high In:Zn ratios to enhance carrier mobility, which also resulted in amorphous IZO via hydrolysis. In our case, annealing at a relatively low temperature of 300 °C results in highly crystalline thin films (see figure 1(c)).

The UV–vis–NIR range optical reflectance of ZnO and AZO thin films and multilayers were also acquired and shown in figure 2. The single layer thin films for both materials exhibit characteristic high transparency, similar to IZO and related transparent amorphous oxide TFTs. With iterative coating of 5 periodic layers to the film, the reflectance increase to ~50% for both materials at wavelengths close to 500 nm. Thin films with 8 and up to 20 layers as a coherent homogeneous QSL of granular and dense sub-structure behaves as a coherent film with a measured thickness proportional to the number of sequential coatings. Reflectance spectra exhibit characteristic wavelength dependent interference from half-wave (reflectance minima) and quarter-wave (reflectance maxima) optical thickness (QWOT) variation. Of importance in these observations is the evidence of dispersion in the reflectance spectra at longer wavelengths from thin films of both materials. At energies below the bandgap, Urbach states, defect absorption, processes involving multiphonon interactions and scattering all increase reflectivity. Urbach and defect absorption is likely, since the sub-band photoluminescence shows several emission features, and TEM data in figure 1 confirms granular features in part of the periodic structure, for films that exhibit a high degree of crystalline orientation as a layer. The broadband reflectance spectra for ZnO and AZO are similar as expected for multilayered systems with period control in layer thickness; spectra are blue-shifted by ~40 nm for AZO compared to ZnO.

Metal oxides used as transparent channel materials in TFTs can be processed by several methods, and the resulting composition and annealing condition influence the amorphous or crystalline nature, which in turn affects electrical properties. In parallel, the optical conductivity is critical for defining the energy range of optimum transparency. In multilayers or QSLs that can have significant influence over carrier mobility and conductivity, it has not yet been established if the transparency is a function of multilayer substructure or morphology. Recently, attempts to remove the dependence of carrier (Hall) mobility were made by developing heterointerfaces between dissimilar oxide semiconductors in the channel material. These interfaces removed the dependence on bulk carrier mobility of each single semiconductor layer—the interfacial carrier mobility was higher. Quasi-superlattice structures [33] using In_2O_3–Ga_2O_3–ZnO–Ga_2O_3–In_2O_3, presumably without interfacial mixing, gave an electronic carrier mobility of $\mu_e > 40\,cm^2\,V^{-1}\,s^{-1}$. As the morphology of our ZnO and AZO materials with homo-interfaces in multilayers are similar, the reflectance data shown in figure 2 confirm that these films behave as continuous, coherent ZnO and AZO films, with wavelength-dependent refractive index consistent with uniphasic, highly uniform thin films, and they exhibit considerable dispersion.

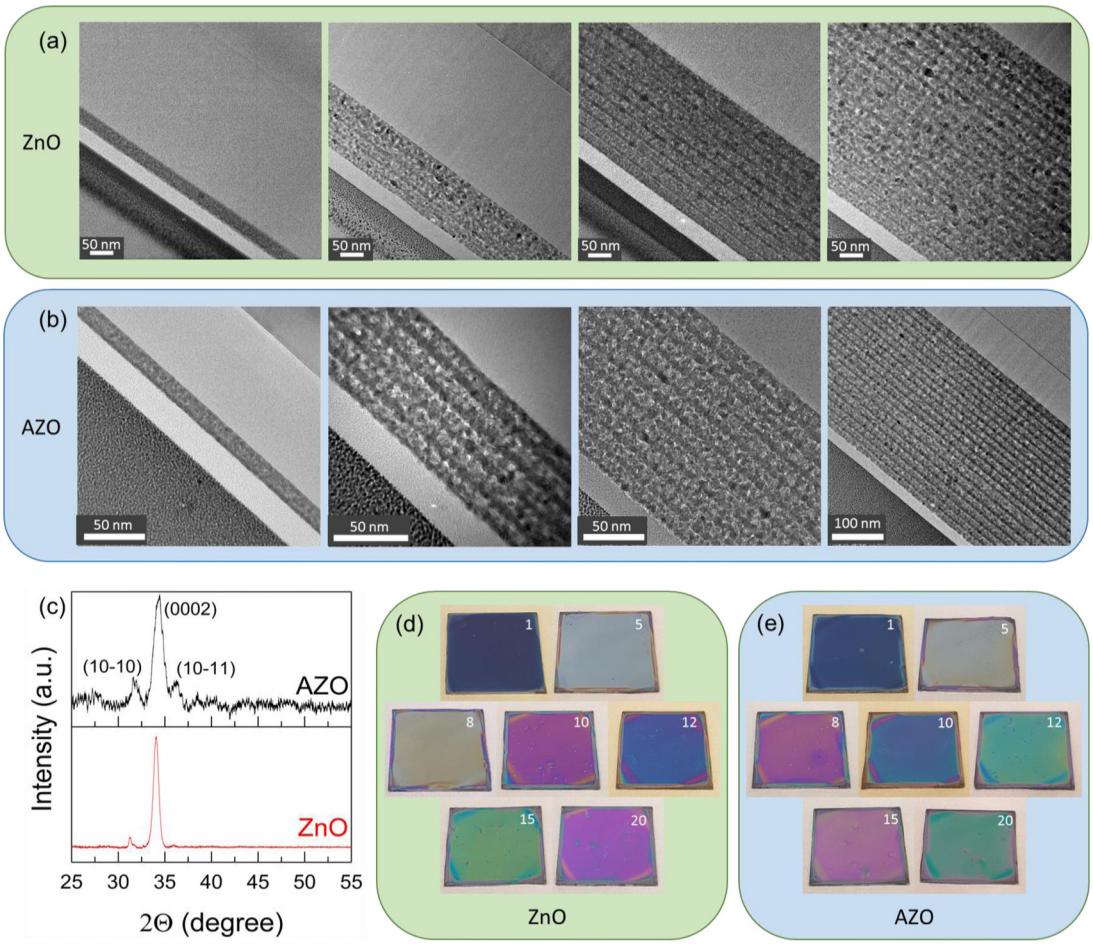


Figure 1. (a) TEM cross-sectional images of 1, 5, 10 and 20 layer ZnO and (b) AZO thin films on SiO_2 covered Si substrates. (c) X-ray diffraction patterns of 20 layer QSL ZnO and AZO samples. (d) Visual comparison of 1–20 layer deposited ZnO and (e) AZO single and QSL thin films highlighting thickness-dependent colour change. The number of iterative deposits is shown inset to each image.

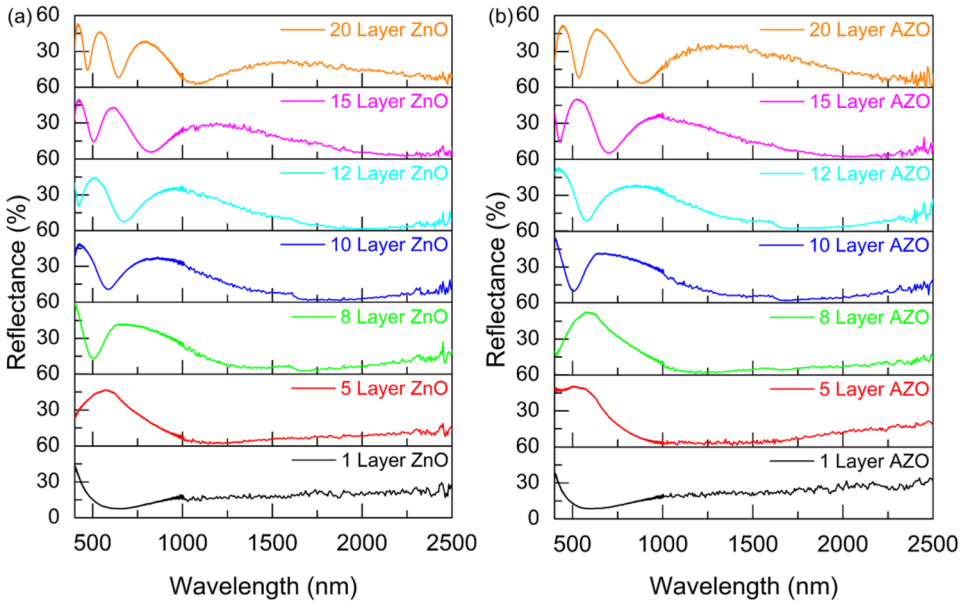


Figure 2. UV–vis–NIR reflectance spectra of 1–20 layer (a) ZnO and (b) AZO single and QSL thin films acquired at angle of incidence, $\theta_i = 45°$.

We adapted a method from thin film optics [34] to determine the effective thickness via examination of the reflectance maxima for all data in figure 2 (see supplementary material) accounting for refractive index contrast and wavelength-dependence, Fresnel reflection and dispersion. For both ZnO and AZO films, the UV–vis–NIR reflectance spectra (between

the band-edge absorption energy and the onset of high reflectivity above the plasma wavelength via the Drude model, given by $\lambda_p = \frac{2\pi c\sqrt{m^* \in_0}}{q\sqrt{n}}$, where m^* and q are the effective mass and charge of an electron, ϵ_0 the high-frequency permittivity of free-space, c is the speed of light in a vacuum, and n is the carrier concentration) capture all phase changes (maxima and minima) to accurately determine the first QWOT. Briefly, for odd orders of reflectance (maxima), the reflectance can be represented as

$$\mathbf{Rf_\lambda} = \frac{\left(nf_\lambda^2 - ns_\lambda\right)^2}{\left(nf_\lambda^2 + ns_\lambda\right)^2} \quad (1)$$

where nf_λ is the effective refractive index at wavelength λ, ns_λ is the refractive index of the thin film at that wavelength, and $\mathbf{Rf_\lambda}$ is the maximum reflectance for the odd order (maximum) at the same wavelength. The refractive index of thin film at the reflectance maxima can be calculated according to:

$$nf_\lambda = ns_\lambda\left(\frac{1+\sqrt{\mathbf{Rf_\lambda}}}{1-\sqrt{\mathbf{Rf_\lambda}}}\right)^{0.5} \quad (2)$$

At order m the phase thickness is $m\pi = \frac{4\pi}{\lambda_m} n_m d$, where λ_m and n_m are the wavelength and refractive index respectively of a specific m^{th} order thus, the thickness of the thin film can be calculated using:

$$\mathrm{d} = \frac{m\lambda_m}{4n_m} \quad (3)$$

The value of n_m is calculated using equation (2), which is the effective refractive index of the thin film at the reflectance maxima that occur at consecutive odd orders. The refractive index of even orders was then calculated using equation (3) above using the film thickness (d) of the lowest odd order maximum.

The optical thickness determined from the reflection data of ZnO and AZO thin films and QSLs are shown in figure 3. The actual film thicknesses were accurately determined from the TEM data in figure 1. In figure 3(a), the variation of optical thickness was acquired for each reflectance maximum, and we observed that the best agreement corresponds to the lowest order reflectance maximum in all cases. Higher order reflectance maxima predict films of lower thickness, and the divergence from actual thickness is less accurate for thicker films of both materials. We quantitatively assessed the relative error in the refractive index and optical thickness via the functional dependence from equations (1) and (2) above, and in all cases (figure 3) the error does not account for the divergence in optical thickness values in dispersive thin films or multilayers of ZnO or AZO. Very accurate optical thickness measurements are possible, and it should allow prediction of other oxide phases formed as thin films from the broadband reflectance spectra, and identification of the effect of thickness on the transparency of TFTs separate to their electrical characteristics, since carrier concentration increases can reduce optical transparency. We do observe that thinner films (single layers and thinner multilayers) for either material

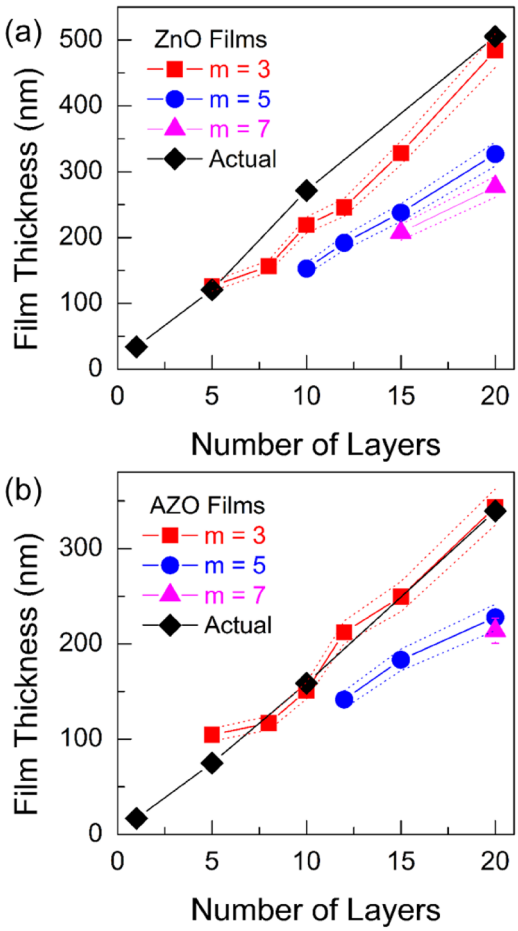


Figure 3. Thickness of thin films measured by TEM (actual) versus calculated optical thickness at multiple reflectance order maxima for (a) ZnO and (b) AZO single layers and QSLs. Solid lines are guides to the eye. Dashed lines represent the margin of error with each calculation for each order m. Readers can refer to the supplementary material for error analysis calculations.

in general give better agreement with the predicted optical thickness for dispersive films (with defect states or scattering contributions) that have wide bandgaps and transparency in the visible region.

While the reflectance and transparency of TFT materials are important for display applications, the angle-dependence of reflectance matters for high density TFT pixel arrays for true colour rendering, for see-through or flexible technologies based on solution-processed TFT materials, or transparent conductive antireflection coatings. We determined the angle-resolved reflectance for 1, 10 and 20 layer ZnO and AZO films and QSL, shown in figure 4. The corresponding spectra are provided in the Supplementary material, figure S1. Reflectance measurements were compared for three common laser wavelengths in the green to red range of the visible spectrum (strong absorption occurs in the blue for wide bandgap materials such as ZnO and AZO).

ZnO thin film TFT materials exhibit a consistent degree of anti-reflection characteristics from 30–60° (~10–12%) for thickness ranging from ~40 nm to 500 nm. At higher angles away from normal incidence, transparency is reduced considerably for any film thickness at 810 nm. The reflectance

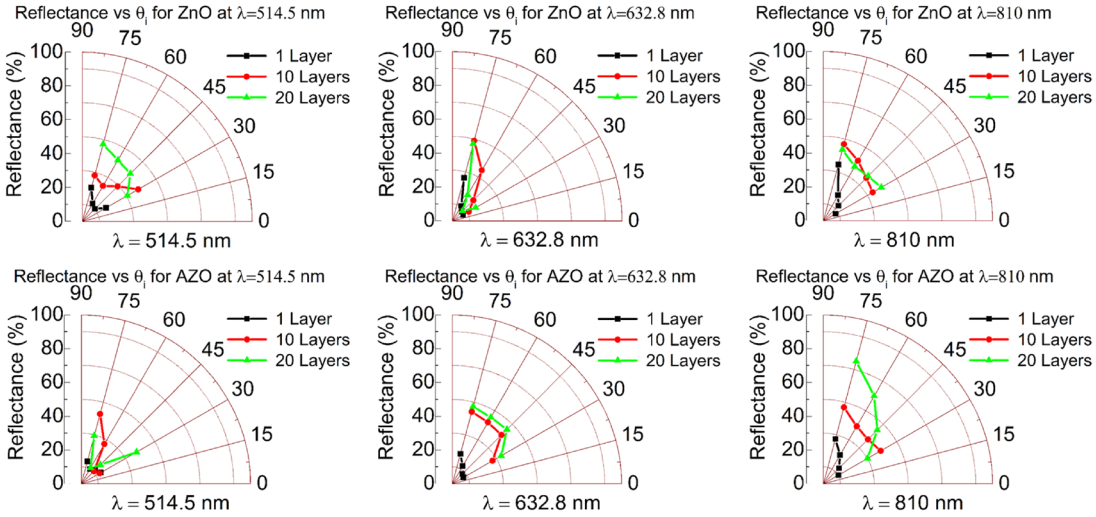


Figure 4. Angle-resolved reflectance of 1, 10 and 20 layer ZnO (top) and AZO QSLs (bottom) at 3 common laser wavelengths (514.5 nm, 632.8 nm and 810 nm).

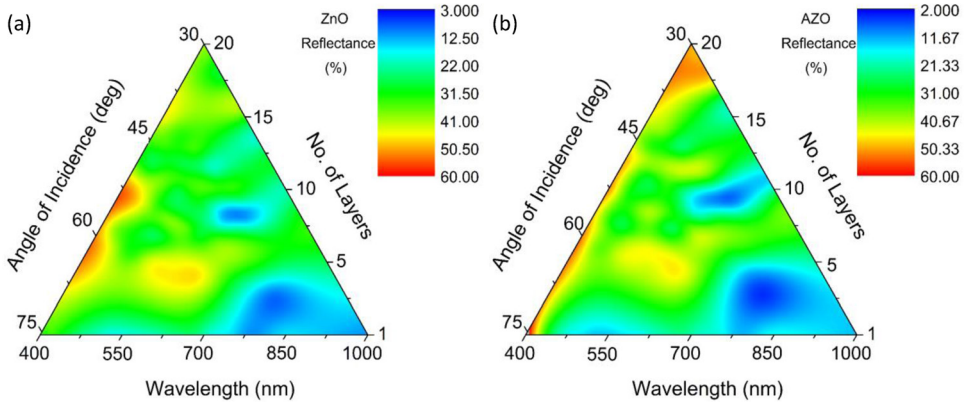


Figure 5. (a) Reflectance intensity mapping as a function of angle of incidence and multilayer thickness (number of layers) in the UV–vis–NIR regions for full sample sets (1–20 layers) of ZnO and (b) AZO thin films. The numbers of layers can be correlated with accurate thickness from figure 3.

of AZO single layer thin films (~18 nm thickness) is <10% from 30 to 75° at 514.5 nm, <6% at 632.8 nm for 30–60°, with greater reflectance observed at higher angles. This effect is also more pronounced at longer wavelengths (810 nm), where reflectance is minimized in thicker films closer to normal incidence.

Figure 5 present all optical reflectance data for all films and QSLs as a function of angle from normal incidence and wavelength. The reflectivity variation with thickness and ZnO versus AZO composition shows some similarity in the variation of minimum reflectance. The number of periodic layers relates to a particular thickness from figure 3. In figure 5, and from analysis in figure 3 and Supplementary materials, the true correlation between optical thickness and actual thickness is not immediately apparent—this work demonstrates that for all thickness for either material, shorter wavelengths are more accurate for thickness determination at the expense of marginally higher reflectance due to dispersion and scattering. However, as a design rule for homo- or hetero QSL type multilayers or thin films for TFTs, diodes, anti-reflection coatings, solar cells and active materials for display technologies, this angle-resolved spectral mapping provides a method for determining comparative angle-resolved transparency (directional reflectance) for thin film materials, and we see that AZO films demonstrate significant reflectivity at shorter wavelengths, that is not related to the onset of the band-edge absorption, but is caused by interference and dispersion in similarly thick films in the visible range. For AZO, this effect is pronounced at higher and lower angles, compared to ZnO multilayers, which provide better anti-reflection characteristics.

Conclusions

This work has shown an approach to determining the optical thickness and directional reflectance of metal oxide (ZnO and AZO thin films and QSLs on oxidized Si). The method is particularly useful for the IGZO, ZnO, AZO, IZO and related classes of crystalline or amorphous oxide semiconductor channel materials in transparent thin film transistors, and other display device and transistor technology applications where directional reflectance/transparency of the materials is also important. Aside from electronic conductivity and its

relationship to the film substructure and band structure, the (angle-resolved) reflectance (between bandgap absorption the plasma frequency) can be determined for single, multi or homogeneous QSL layers of oxide materials and used to define the optical thickness for dispersive or lossy thin films with known effective refractive index.

Of importance is the observation that thin films with internal grain structure behave as continuous films, but the true optical thickness is determined at lower wavelengths for all thickness (40–500 nm) investigated, for both ZnO or AZO. The reflectance or transparency is non-optimum in the transparent region for such films. Angle-resolved investigation of reflectance variation shows that both single and QSL ZnO and AZO exhibit directional reflectance that is thickness dependent, and the thinnest films at lower angle minimize reflectance. Internal granularity and dispersion increase reflectance with angle considerably for such materials and homogeneous QSLs, which is a consideration for TFT channel material design as sub structure, composition as well as angle-resolved spectral reflectance may determine the optimum mobility, conductivity and transparency characteristics.

Acknowledgments

DB acknowledges the support of the Irish Research Council under award GOIPG/2014/206. COD acknowledges support from Science Foundation Ireland (SFI) through the SFI Technology Innovation and Development Award 2015 under contract 15/TIDA/2893 and by a research grant from SFI under grant Number 14/IA/2581.

References

[1] Fortunato E, Barquinha P, Pimentel A, Gonçalves A, Marques A, Pereira L and Martins R 2005 *Thin Solid Films* **487** 205
[2] Ginley D S and Bright C 2000 *MRS Bull.* **25** 15
[3] O'Dwyer C, Szachowicz M, Visimberga G, Lavayen V, Newcomb S B and Torres C M S 2009 *Nat. Nanotechnol.* **4** 239
[4] King P D C and Veal T D 2011 *J. Phys.: Condens. Matter.* **23** 334214
[5] Lee Y J, Ruby D S, Peters D W, McKenzie B B and Hsu J W P 2008 *Nano. Lett.* **8** 1501
[6] Raut H K, Ganesh V A, Nair A S and Ramakrishna S 2011 *Energy Environ. Sci.* **4** 3779
[7] Banger K K, Yamashita Y, Mori K, Peterson R L, Leedham T, Rickard J and Sirringhaus H 2011 *Nat. Mater.* **10** 45
[8] Chen C P, Chen Y D and Chuang S C 2011 *Adv. Mater.* **23** 3859
[9] Chou T P, Zhang Q, Fryxell G E and Cao G 2007 *Adv. Mater.* **19** 2588
[10] Granqvist C G 2014 *Thin Solid Films* **564** 1
[11] Özgür Ü, Alivov Ya I, Liu C, Teke A, Reshchikov M A, Dogan S, Avrutin V, Cho S-J and Morkoç H 2005 *J. Appl. Phys.* **98** 041301
[12] Look D C 2006 *Zinc Oxide Bulk, Thin Films and Nanostructures* ed C Jagadish and S J Pearton (Oxford: Elsevier) p 21
[13] Lyubchyk A, Vicente A, Alves P U, Catela B, Soule B, Mateus T, Mendes M J, Águas H, Fortunato E and Martins R 2016 *Phys. Status Solidi* a **213** 2317
[14] Hamberg I, Granqvist C G, Berggren K F, Sernelius B E and Engström L 1985 *Sol. Energy. Mater.* **12** 479
[15] Song K, Noh J, Jun T, Jung Y, Kang H Y and Moon J 2010 *Adv. Mater.* **22** 4308
[16] Yu X, Marks T J and Facchetti A 2016 *Nat. Mater.* **15** 383
[17] Lyubchyk A, Vicente A, Soule B, Alves P U, Mateus T, Mendes M J, Águas H, Fortunato E and Martins R 2016 *Adv. Electron. Mater.* **2** 1500287
[18] Fortunato E M C, Barquinha P M C, Pimentel A C M B G, Gonçalves A M F, Marques A J S, Pereira L M N and Martins R F P 2005 *Adv. Mater.* **17** 590
[19] Al-Kuhaili M F, Alade I O and Durrani S M A 2014 *Opt. Mater. Express* **4** 2323
[20] Shan F K and Yu Y S 2004 *J. Eur. Ceram. Soc.* **24** 1869
[21] Liu G, Liu A, Zhu H, Shin B, Fortunato E, Martins R, Wang Y and Shan F 2015 *Adv. Funct. Mater.* **25** 2564
[22] Armelao L, Fabrizio M, Gialanella S and Zordan F 2001 *Thin Solid Films* **394** 89
[23] Nomura K, Ohta H, Takagi A, Kamiya T, Hirano M and Hosono H 2004 *Nature* **432** 488
[24] Fortunato E, Gonçalves A, Pimentel A, Barquinha P, Gonçalves G, Pereira L, Ferreira I and Martins R 2009 *Appl. Phys.* A **96** 197
[25] Li M C, Kuo C C, Peng S H, Chen S H and Lee C C 2011 *Appl. Opt.* **50** C197
[26] Li X D, Chen T P, Liu Y and Leong K C 2014 *Opt. Express* **22** 23086
[27] Sernelius B E, Berggren K F, Jin Z C, Hamberg I and Granqvist C G 1988 *Phys. Rev.* B **37** 10244
[28] Glynn C and O'Dwyer C 2017 *Adv. Mater. Interfaces* **4** 1600610
[29] Jo J W, Kim J, Kim K T, Kang J G, Kim M G, Kim K H, Ko H, Kim Y H and Park S K 2015 *Adv. Mater.* **27** 1182
[30] Pasquarelli R M, Ginley D S and O'Hayre R 2011 *Chem. Soc. Rev.* **40** 5406
[31] Glynn C, Aureau D, Collins G, O'Hanlon S, Etcheberry A and O'Dwyer C 2015 *Nanoscale* **7** 20227
[32] Kinsey N, DeVault C, Kim J, Ferrera M, Shalaev V M and Boltasseva A 2015 *Optica* **2** 616
[33] Lin Y H *et al* 2015 *Adv. Sci.* **2** 1500058
[34] Angus MacLeod H 2010 *Thin-Film Optical Filters* 4th edn (Boca Raton, FL: CRC Press)